ORIGINAL PAPER

Experimental and DFT computational studies on 5-benzyl-4-(3,4-dimethoxyphenethyl)-2H-1,2,4-triazol-3(4H)-one

Hasan Tanak · Yavuz Köysal · Metin Yavuz · Orhan Büyükgüngör · Kemal Sancak

Abstract The triazole compound, 5-benzyl-4-(3,4-dime-thoxyphenethyl)-2H-1,2,4-triazol-3(4H)-one, has been synthesized and characterized by ^{1}H-NMR, ^{13}C-NMR, IR, and X-ray single-crystal determination. The compound crystallizes in the monoclinic space group $P2_1$ with a= 11.8844(3) Å, b=17.5087(4) Å, c=17.3648(6) Å, β= 99.990(2)° and Z=8. In addition to the molecular geometry from X-ray experiment, the molecular geometry, vibrational frequencies and gauge including atomic orbital (GIAO) ^{1}H- and ^{13}C-NMR chemical shift values of the title compound in the ground state have been calculated using the density functional method (B3LYP) with 6-31G (d,p) basis set. The calculated results show that the optimized geometries can well reproduce the crystal structure and the theoretical vibrational frequencies and chemical shift values show good agreement with experimental ones. Besides, molecular electrostatic potential (MEP), natural bond orbital (NBO), and frontier molecular orbitals (FMO) analysis of the title compound were performed by the B3LYP/6-31G(d,p) method.

H. Tanak (✉) · M. Yavuz · O. Büyükgüngör
Department of Physics, Faculty of Arts and Sciences,
Ondokuz Mayıs University,
55139 Kurupelit, Samsun, Turkey
e-mail: htanak@omu.edu.tr

Y. Köysal
Samsun Vocational School, Ondokuz Mayıs University,
55139 Kurupelit, Samsun, Turkey

K. Sancak
Department of Chemistry, Faculty of Arts and Sciences,
Karadeniz Technical University,
61080 Trabzon, Turkey

Introduction

By means of increasing development of computational chemistry in the past decade, the research of theoretical modeling of drug design, functional material design, *etc*., has become much more mature. Many important chemical and physical properties of biological and chemical systems can be predicted from the first principles by various computational techniques [1]. In recent years, density functional theory (DFT) has been a shooting star in theoretical modeling. The development of better and better exchange-correlation functionals made it possible to calculate many molecular properties with comparable accuracies to traditional correlated *ab initio* methods, with more favorable computational costs [2]. Literature survey revealed that the DFT has a great accuracy in reproducing the experimental values of geometry, dipol moment, vibrational frequency, *etc*. [3–9].

The chemistry and structure of heterocyclic compounds has been an interesting field of study for a long time. The synthesis of 1,2,4-triazoles and investigation of their chemical and biological behavior have gained more importance in recent decades for biological, medicinal, and agricultural reasons. 1,2,4-Triazole and 1,2,4-triazol-3-one are reported to exhibit a broad spectrum of biological activities such as antifungal, antimicrobial, hypoglycemic, antihypertensive, analgesic, antiparasitic, antiviral, *anti*-inflammatory, antitumor, and *anti*-HIV properties [10–16]. Substituted 1,2,4-triazoles were also applied as ligands to obtain metal complexes with specific properties [17–19].

The literature concerning the 1,2,3- and 1,2,4-triazoles is rich and the papers published cover such subjects as crystal structure determination [20, 21], *ab initio* and DFT calculations on the tautomerism and protonation sites [22–27], vibrational characteristics and photochemical transformations [28–33], and thermal decomposition products [34–36]. Many reports appeared on the synthesis and characterization of novel triazole containing organic [37–39] or metal coordination compounds [40–43] including spin-crossover materials [44, 45].

In this paper, we wish to report the synthesis, characterization and crystal structure of the triazole compound, 5-benzyl-4-(3,4-dimethoxyphenethyl)-2H-1,2,4-triazol-3 (4H)-one, as well as the theoretical studies on it by using the DFT/B3LYP/6-31G(d,p) method. The properties of the structural geometry, molecular electrostatic potential (MEP), natural bond orbitals (NBO), frontier molecular orbitals (FMO), and the thermodynamic properties for the title compound at the B3LYP/6-31G(d,p) level were studied. We also make comparisons between experiments and calculations.

Experimental

Ethyl 2-[1-ethoxy-2-(phenyl)ethylidene]hydrazine carboxylates **(1)** (10 mmol) together with 2-(3,4 dimethoxyphenyl) ethylamin **(2)** (10 mmol) were heated without solvent in a sealed tube for 2 h at 160 °C. Then, the mixture was cooled to r.t. and a solid formed. The crude product was recrystallized using acetone/petroleum ether (1:2) to afford the desired compound **(3)** (see Scheme 1). Yield: 200 mg (67%). Colorless crystals. M.P. 133-134°C. The IR spectra were recorded in the 4000-400 cm^{-1} region using KBr pellets on a Schmadzu FTIR-8900 spectrophotometer. The ^{1}H-, and ^{13}C-nuclear magnetic resonance spectra were recorded on a Varian-Mercury 400 MHz spectrometer. IR (KBr, cm^{-1}): 3194 (NH), 1577 (C=N); 1714 (C=O). ^{1}H-NMR (200 MHz, DMSO$_{d-6}$): 2.50 (s, 2H, N-CH$_2$-C$\underline{H}_2$); 3.56 (s, 4H, Ph-CH$_2$ +N-CH$_2$); 3.71 (s, 6H, OCH$_3$); 6.57–6.59 (m, 2H, arom.H);

6.85 (s, 1H, arom.H); 7.15–7.35 (m, 5H, arom.H). ^{13}C NMR (200 MHz, DMSO$_{d-6}$): 31.16 (N-CH$_2$-$\underline{C}$H$_2$); 33.42 (N-$\underline{C}$H$_2$); 42.01 (Ph-$\underline{C}$H$_2$); 55.32 (OCH$_3$); arom. C [111.67 (CH), 112.18 (CH), 120.50 (CH), 126.83(CH), 128.51 (CH), 128.55(CH), 130.05 (C), 137.27 (C), 146.19 (C), 147.36 (C), 148.49 (C)]; 148.49 (C=N); 154.88 (C=O).

Crystal data for the title compound

CCDC 727857, C$_{19}$H$_{21}$N$_3$O$_3$, M_w=339.39, monoclinic, space group $P2_1$; Z=8, a=11.8844(3) Å, b=17.5087(4) Å, c=17.3648(6) Å, β=99.990(2)° and V=3558.49(13) Å^3, F(000)=1439.7, D_x=1.267 g/cm^3.

Computational methods

The calculations of geometrical parameters were performed using the Gaussian 03 program package [46] and B3LYP (Becke's three parameter hybrid functional using the LYP correlation functional) approach in conjunction with the 6-31G(d,p) basis set. For modeling, the initial guess of the title compound was first obtained from the X-ray coordinates. The harmonic vibrational frequencies were calculated at the same level of theory for the optimized structure C and the obtained frequencies were scaled by 0.9627 [47]. By using Gauss-View molecular visualization program [48], the vibrational bands assignments have been made. The geometry of the title compound, together with that of tetramethylsilane (TMS) is fully optimized. ^{1}H and ^{13}C NMR chemical shifts were calculated using the standard GIAO/B3LYP/6-31G(d,p) (gauge-independent atomic orbital) approach [49, 50] with the Gaussian 03 program package. The ^{1}H and ^{13}C NMR chemical shifts are converted to the TMS scale by subtracting the calculated absolute chemical shielding of TMS whose values are 32.01 and 184.38 ppm for B3LYP/6-31G(d,p), respectively. To investigate the reactive sites of the title compound the molecular electrostatic potential were evaluated using the B3LYP/6-31G(d,p) method. Molecular electrostatic potential,

Scheme 1 Synthesis scheme of the title compound
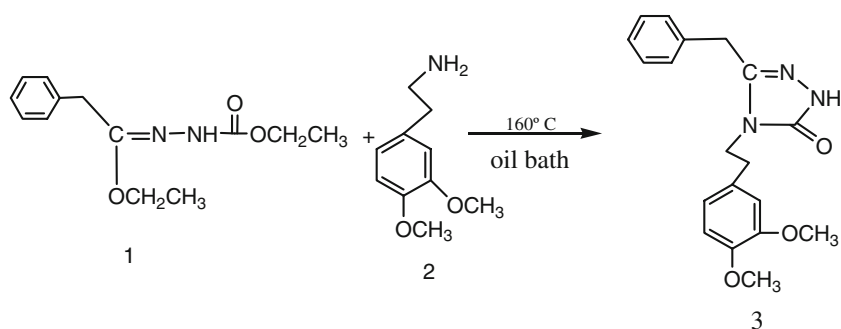
V(r), at a given point r(x,y,z) in the vicinity of a molecule, is defined in terms of the interaction energy between the electrical charge generated from the molecule electrons and nuclei and a positive test charge (a proton) located at r. For the system studied the V(r) values were calculated as described previously using the equation [51],

$$V(r) = \sum Z_A \Big/ |R_A - r| - \int \rho(r') \Big/ |r' - r| d^3 r' \qquad (1)$$

where Z_A is the charge of nucleus A, located at R_A, $\rho(r')$ is the electronic density function of the molecule, and r' is the dummy integration variable. The thermodynamic properties of the title compound at different temperatures were calculated on the basis of vibrational analyses. In addition, natural bond orbitals (NBO) and frontier molecular orbitals (FMO) were performed with B3LYP/6-31G(d,p) the optimized structure.

Results and discussion

Crystal structure

The title compound, an Ortep-3 [52] view of which is shown in Fig. 1, crystallizes in the monoclinic space group

$P2_1$ with $Z=8$ in the unit cell. The asymmetric unit contains four independent molecules (A, B, C and D). In the title compound, each molecule contains three, viz. the 1,2,4-triazole ring, the dimethoxyphenyl ring, and benzyl ring. In the molecular structure, two benzyl rings are bridged by 1,2,4-triazole ring system. The minimum dihedral angle between the triazole and dimethoxyphenyl for the independent molecules is 5.93(1)°, is indicate that these rings are almost planar while six membered rings are nearly perpendicular to each other. The maximum dihedral angle is 85.7(1)° in the four molecules (A, B, C, and D) in the asymmetric unit. The torsion angles (N1-C10-C11-C12) for A, B, C, and D molecules are 179.0(2)°, 177.6(2)°, 178.3(2)°, and -180.0(2)°, respectively, shows that for the title compound, the side chain conformation induced by the *anti* conformations. For all the independent molecules, the five membered triazole rings have the same planar geometry. The interatomic distances within the triazole ring are not equal. The C8=N3 of all independent molecules are double bonds and shorter than the conjugated C8-N1 bonds. The molecular geometry of the triazole ring is in agreement with the values of structure 4-(3-Methoxy-phenyl)-3-[2-(4-methoxyphenyl)ethyl]-1H-1,2,4-triazol-5 (4H)-one [53].
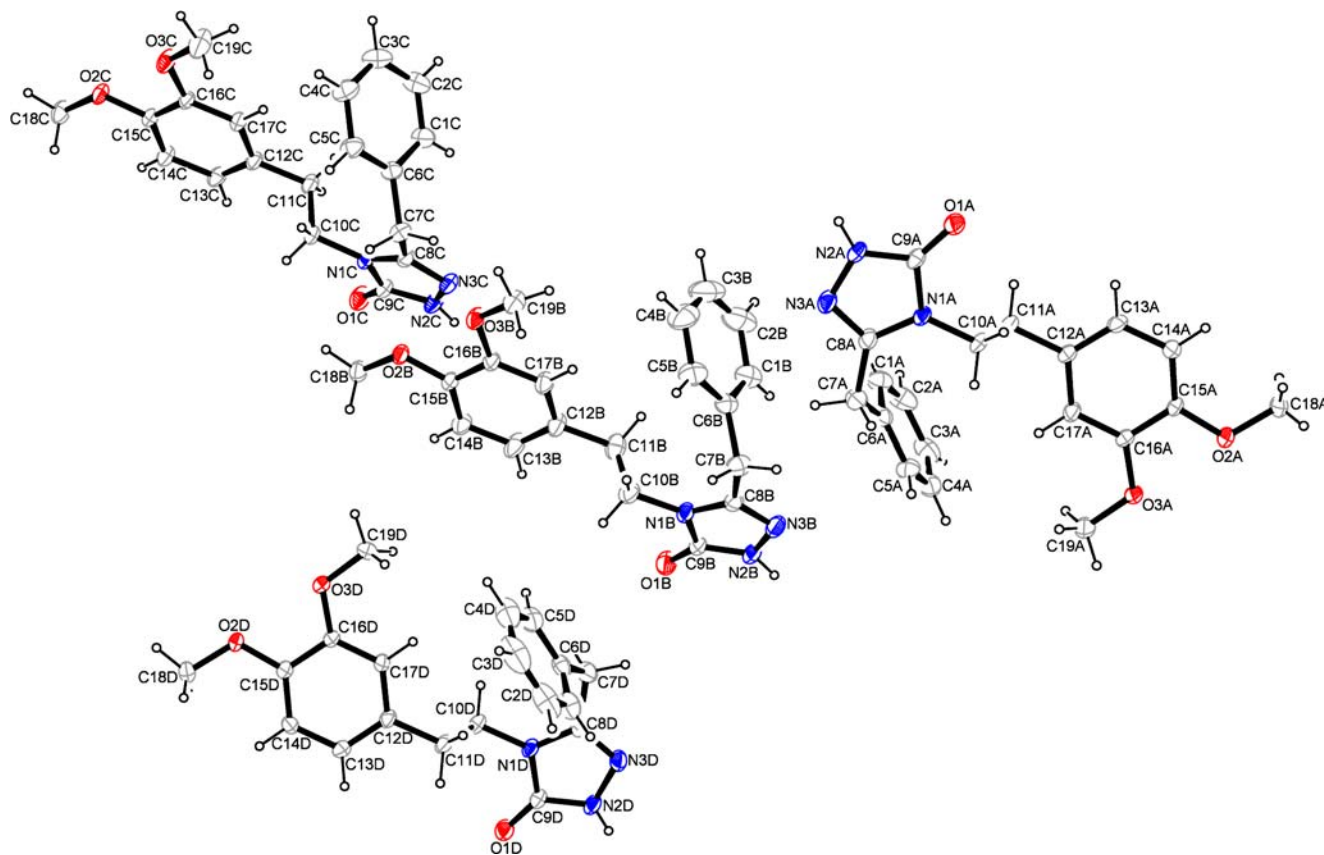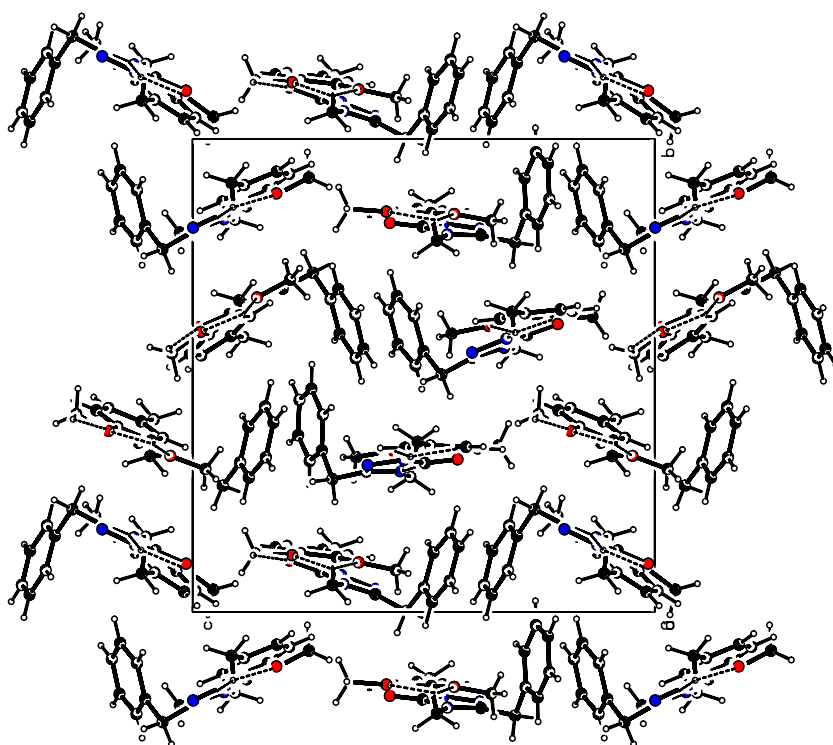

Fig. 1 Ortep 3 diagram of the title compound

Fig. 2 Packing diagram of the title compound along the a axis

The crystal structure is stabilized by N-H···O and C-H···O intermolecular contacts which link the molecules into discrete pairs across crystallographic centers of symmetry, shown in Fig. 2. N2B-H8B, N2C-H8C, and N2D-H8D bonds forms a bifurcated contact with two acceptors of methoxy oxygen, namely O2B-O3B, O2C-O3C and O2D-

O3D [N2B-H8B···O2B[i], N2B-H8B···O3B[i], N2C-H8C···O2C[i], N2C-H8C···O3C[i], N2D-H8D···O2D[i], N2D-H8D···O3D[i], symmetry code: (i) x+1, y, z]. The bifurcated contact explains the relative large H···A distances and the relative small D-H···A angles [54]. The other important contacts are C18A-H22A···O1A[i], C18C-H22C···O1C[ii] and C18D-H22D···O1D[ii] (symmetry code: (ii) x-1, y, z). There is also π-π contact between the triazole rings N1A-C9A and N1D-C9D [centroid-centroid distance is 3.44(2) Å]. C-H···π contacts are also found in between the phenethyl ring and methyl groups of their methoxy substituent, and between triazole ring and methyl groups of their methoxy substituent (Table 1).

Theoretical structures

The optimized parameters (bond lengths, bond angles, and dihedral angles) of the title compound have been obtained by using B3LYP/6-31G(d,p) method for all independent molecules. These results are listed in Table 2 and compared with the experimental data of the title compound. When the X-ray structure of the title compound is compared with its optimized counterparts (see Fig. 3), conformational discrepancies are observed between them. The most remarkable discrepancies exist in the orientation of the dimethoxyphenyl ring of the title compound. Although the dihedral angles between the five-membered 1,2,4-triazole and the dimethoxyphenyl rings for the independent molecules A, B, C, and D are 6.4(1)°, 9.18(1)°, 13.71

Table 1 Hydrogen-bond geometry (Å, °)

D-H···A	D-H	H···A	D···A	D-H···A
N2C-H8C···O2C[i]	0.90(4)	2.15(4)	2.997(3)	157(3)
N2C-H8C···O3C[i]	0.90(4)	2.28(4)	2.959(3)	133(3)
N2B-H8B···O3B[i]	0.89(4)	2.13(4)	2.915(3)	148(3)
N2B-H8B···O2B[i]	0.89(4)	2.39(3)	3.148(3)	143(3)
N2D-H8D···O3D[i]	0.81(2)	2.37(2)	3.031(3)	140(2)
N2D-H8D···O2D[i]	0.81(2)	2.31(3)	3.036(3)	150(2)
C18A-H22A···O1A[i]	0.96	2.54	3.345(3)	141.4
C18C-H22C···O1C[ii]	0.96	2.56	3.389(4)	144.2
C18D-H22D···O1D[ii]	0.96	2.45	3.273(4)	144.3
C18A-H20A···Cg(9)[iii]	0.98	2.86	3.804(4)	169
C18B-H20B···Cg(7)[iv]	0.93	2.91	3.673(4)	138
C18D-H18D···Cg(1)[v]	0.90	2.89	3.814(4)	161
C19D-H21D···Cg(3)[vi]	0.88	2.99	3.820(4)	145

Symmetry codes: (i) x+1,y,z ; (ii) x-1,y,z ; (iii) 1-x,1/2+y,1-z ; (iv) -x,1/2+y,1-z ; (v) -x,-1/2+y,-z ; (vi) x,y,z. Cg(9), Cg(7), Cg(1) and Cg(3) is the centroids of the C12C-C17C, N1C-C9C, N1A-C9A and C12A-C17A rings, respectively

Table 2 Selected molecular structure parameters

Parameters	Experiment				DFT/6-31G(d,p)			
	A	B	C	D	A	B	C	D
Bond lengths (Å)								
C6-C7	1.520(4)	1.508(4)	1.514(4)	1.510(4)	1.52281	1.52281	1.52281	1.52281
C7-C8	1.486(4)	1.497(4)	1.487(4)	1.489(4)	1.49717	1.49717	1.49717	1.49716
C8-N3	1.305(3)	1.295(4)	1.305(3)	1.300(3)	1.30521	1.30522	1.30521	1.30521
C8-N1	1.369(3)	1.360(3)	1.363(3)	1.361(3)	1.38168	1.38167	1.38168	1.38168
C9-O1	1.211(3)	1.223(3)	1.219(3)	1.226(3)	1.22259	1.22259	1.22259	1.22259
C9-N2	1.360(3)	1.338(3)	1.352(4)	1.357(3)	1.37629	1.37629	1.37629	1.37629
C9-N1	1.388(3)	1.389(3)	1.391(3)	1.381(3)	1.40367	1.40367	1.40366	1.40366
C10-N1	1.458(3)	1.465(3)	1.464(3)	1.459(3)	1.45928	1.45927	1.45928	1.45928
C10-C11	1.523(4)	1.481(4)	1.514(4)	1.518(4)	1.54201	1.54201	1.54201	1.542
C11-C12	1.507(4)	1.525(4)	1.515(4)	1.509(4)	1.51255	1.51254	1.51255	1.51255
C15-O2	1.375(3)	1.369(3)	1.370(3)	1.375(3)	1.36425	1.36425	1.36425	1.36425
C15-C16	1.390(4)	1.402(4)	1.388(4)	1.394(4)	1.41805	1.41806	1.41805	1.41804
C16-O3	1.373(3)	1.368(3)	1.368(3)	1.377(3)	1.36467	1.36467	1.36467	1.36467
C18-O2	1.421(3)	1.438(3)	1.432(3)	1.412(3)	1.41694	1.41694	1.41694	1.41694
C19-O3	1.420(3)	1.418(3)	1.426(4)	1.421(3)	1.41624	1.41623	1.41624	1.41624
N2-N3	1.378(3)	1.388(3)	1.391(3)	1.372(3)	1.37882	1.37881	1.37881	1.37882
Bond angles (°)								
C1-C6-C7	121.8(3)	121.7(3)	121.4(3)	121.0(3)	120.725	120.724	120.726	120.727
C8-C7-C6	115.1(3)	115.2(3)	116.2(2)	113.5(3)	115.207	115.207	115.208	115.208
N3-C8-N1	111.2(2)	111.8(2)	111.8(2)	111.7(2)	111.848	111.847	111.847	111.848
N3-C8-C7	123.6(3)	123.8(3)	123.6(3)	124.7(3)	122.768	122.767	122.769	122.770
O1-C9-N2	130.1(3)	129.2(3)	130.2(3)	129.9(3)	130.329	130.329	130.329	130.329
N1-C10-C11	113.2(2)	110.0(3)	112.0(2)	112.3(2)	112.610	112.610	112.610	112.609
C12-C11-C10	110.7(2)	113.5(3)	110.8(2)	112.2(2)	111.642	111.643	111.642	111.641
C13-C12-C11	121.3(2)	121.7(3)	121.8(3)	121.8(2)	121.040	121.043	121.041	121.040
O2-C15-C16	115.1(2)	114.9(2)	115.6(2)	116.0(2)	115.605	115.604	115.605	115.605
O3-C16-C15	114.9(2)	115.9(2)	114.3(2)	114.3(2)	115.417	115.416	115.417	115.417
C15-O2-C18	117.7(2)	117.4(2)	118.3(2)	118.5(2)	117.789	117.789	117.789	117.790
C16-O3-C19	117.8(2)	117.7(2)	118.2(2)	117.5(2)	117.886	117.887	117.886	117.886
Torsion angles (°)								
C1-C6-C7-C8	−44.1(4)	−45.7(4)	−46.9(4)	45.7(4)	−46.619	−46.596	−46.583	46.548
C6-C7-C8-N3	122.8(3)	113.3(3)	118.4(3)	−114.5(3)	112.782	112.786	112.796	−112.793
C6-C7-C8-N1	−59.6(4)	−67.3(4)	−64.7(4)	64.9(4)	−68.428	−68.420	−68.413	68.411
N1-C10-C11-C12	179.0(2)	177.6(2)	178.3(2)	−180.0(2)	178.497	178.507	178.511	−178.525
C10-C11-C12-C13	−103.6(3)	−92.8(4)	−86.6(4)	113.9(3)	−86.117	−86.303	−86.124	86.085
C15-C16-O3-C19	−177(3)	170(3)	174.4(3)	175.4(3)	−178.726	−178.693	−178.709	178.704
C16-C15-O2-C18	173.9(3)	177.1(2)	−176.5(2)	174.4(3)	−179.994	179.997	179.988	−179.99

(1)°, and 12.41(1)° in X-ray, in optimized structures the corresponding angles are 18.83°, 18.6°, 18.39°, and 18.67°, respectively. Another difference in the optimized structures is observed in the relative orientation of the benzyl and triazole rings. The benzyl ring is almost perpendicular to the 1,2,4-triazole group for A, B, C, and D molecules, with dihedral angles of 85.01(1)°, 88.73(1)°, 88.91(1)°, and 87.69(1)° for X-ray, whereas the these angles have been calculated as 87.37°, 87.26°, 86.91°, and 87.3° for B3LYP, respectively.

As seen from Table 2, most of the optimized bond lengths are slightly longer than the experimental values.
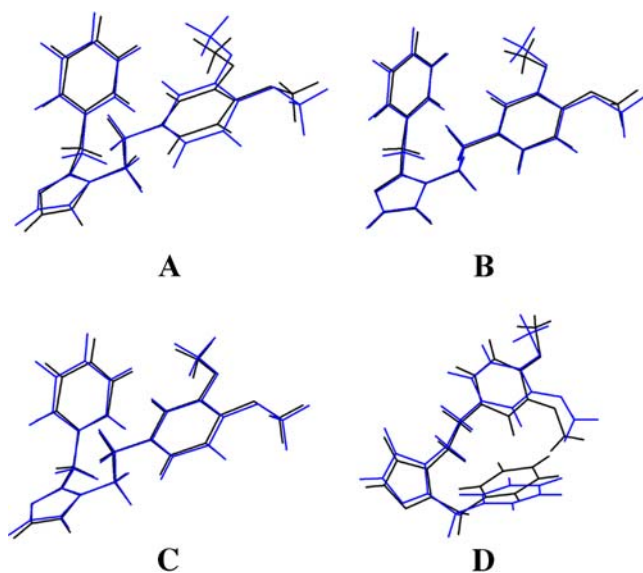
Fig. 3 Atom-by-atom superimposition of the calculated structures (blue) on the X-ray structure (black) for molecules A, B, C, and D

The C8=N3 bond length of the 1,2,4 triazole ring for A, B, C, and D molecules are 1.305(3), 1.295(4), 1.305(3), and 1.300(3) Å in X-ray structure, whereas the corresponding values are 1.30521, 1.30522, 1.30521, and 1.30521Å in optimized geometries for B3LYP, respectively. The C=N bond length is similar to those found in related compounds already studied [55, 56].

A global comparison, by superimposing the molecular skeletons obtained from X-ray diffraction and the theoretical calculations atom by atom was done (Fig. 3) and the RMSE values 0.4822, 0.3917, 0.2074, and 0.7198Å were obtained for A,B,C, and D molecules, respectively.

According to this results, the lowest RMSE value is obtained for molecule C and the geometry obtained from this molecule coincides better with the crystalline structure than other independent molecules. For that reason, to calculate other parameters such as vibrational frequencies, molecular electrostatic potential (MEP), natural bond orbitals (NBO), and thermodynamic properties we used the obtained geometry from molecule C.

IR spectroscopy

Harmonic vibrational frequencies of the title compound were calculated by using DFT method with 6-31G(d,p) basis set. By using Gauss-View molecular visualization program, the vibrational bands assignments have been made. In order to facilitate assignment of the observed peaks we have analyzed vibrational frequencies and compared our calculation of the title compound with their experimental results and showed them in Table 1.

The experimental N-H stretching mode were observed at 3340.51 cm^{-1}, that have been calculated at 3566.67 cm^{-1}. In the triazole, the N-H stretching mode were observed to be 3448 cm^{-1} [57] and 3240 cm^{-1} [58] as experimentally, and 3483 cm^{-1}for B3LYP/6-311G(d,p) level [58], and 3332 cm^{-1} [59] for B3LYP/6-31G(d). These results indicated some band shifts with regard to the different substituent-triazole ring. The C-H aromatic stretching mode was observed to be 3065.93 cm^{-1} experimentally, while they have been calculated at 3077.77 cm^{-1}. The bands at 2948.45 and 2832.55 cm^{-1} correspond to the asymmetric and symmetric stretching CH3 modes, respectively. The calculated bands at 2956.61 and 2898.07 cm^{-1} are ca. shifted 5–70 cm^{-1} toward higher wavenumbers. The stretching C=O vibration gives rise to a band in the infrared experimental spectrum at 1714.04 cm^{-1}, while the calculated value is predicted 51.85 cm^{-1} lower, at 1765.89 cm^{-1}. The experimental C=C and C=N stretch bands were observed at 1624.77 and 1576.78 cm^{-1}, which have been calculated at 1598.14 and 1569.19 cm^{-1}, respectively. The other calculated vibrational frequencies can be seen in Table 3.

To make a comparison with the experimental observation, we present correlation graphics in Fig. 4 based on the calculations. As we can seen from correlation graphics in Fig. 4 experimental fundamentals are found to have a good correlation with calculations. Besides, the vibrational frequencies calculated by DFT method are more compatible to experimental values with the exception of N-H stretching mode. In our results, the N-H stretching mode is estimated with the ~ 7.0 % error in the average for B3LYP levels. The other modes are estimated in the smaller error range.

NMR spectroscopy

GIAO ^{1}H and ^{13}C chemical shift values (with respect to TMS) have been calculated using the B3LYP method with 6-31G(d,p) basis set and generally compared to the experimental ^{1}H and ^{13}C chemical shift values. The results of this calculations are tabulated in Table 4. We have calculated ^{1}H chemical shift values (with respect to TMS) of 7.58-1.31 ppm at B3LYP/6-31G(d,p) level, whereas the experimental results are observed to be 7.35-2.5 ppm. The benzyl protons resonate at 7.15–7.35 ppm multiplet experimentally, that have been calculated at 7.42–7.45 ppm. The OCH3 protons of the title compound gave a singlet at 3.71 ppm. This statement has been calculated 3.36–3.95 ppm at B3LYP level. The singlet observed at 3.56 ppm is assigned to C(7)H2 and C(10)H2 groups, that have been calculated at 3.06–3.95 ppm. In different substituent-1,2,4-triazole, the H chemical shift of N-H were observed to be 11.33–13.56 ppm [60]. This chemical shift has been calculated at 7.38 ppm.

Table 3 Comparison of the experimental and calculated vibrational frequencies (cm^{-1})

Assignments [a]	Experiment	B3LYP/6-31G(d,p)
ν(NH)	3340.51	3565.67
ν_{ring}(CH)	3065.93	3077.77
ν_{as}(CH)	3026.50	3022.22
ν_{as}(CH$_3$)	2948.45	2956.61
ν_s(CH$_3$)	2832.55	2898.07
ν(C=O)	1714.04	1765.89
ν(C=C)	1624.77	1598.14
ν(C=N)	1576.78	1569.19
γ_{ring}(CH)+ω(CH$_3$)	1514.94	1507.97
γ_{ring}(CH)	1495.36	1481.44
γ_{ring}(CH)+α(CH)	1463.98	1448.84
α (CH)+ν(C-N)+γ_{ring}(CH)	1431.11	1416.86
ω(CH$_2$-CH$_2$)	1365.54	1352
ν(C-N)+δ(CH)+ν_{ring}(C-C)	1339.17	1337
γ_{ring}(CH)+ (ring)+ν(C-N)	1260.35	1264.33
γ_{ring}(CH)+ω(CH)+ω (CH$_3$)	1233.27	1229.69
γ_{ring}(CH)+δ (CH)	1196.15	1199.09
γ_{ring}(CH)+ω(CH$_3$)+δ(CH)	1156.20	1157.29
γ_{ring}(CH)+ω(CH)+ω (CH$_3$)	1136.48	1150.24
γ(NH)+γ(CH)+ν(C-N)+ω (CH$_3$)	1069.94	1047.56
γ(NH)+δ(CH)+ν(C-O)	1016.08	1026.54
ω(CH$_2$-CH$_2$)	977.76	995.59
θ(ring)+β(CH)	939.75	925.62
ω_{ring}(CH)	861.77	842.5
θ(ring)+ω $_{ring}$(CH)	794.22	796.37
θ(triazole ring)+ω $_{ring}$(CH)	770.08	774.56
θ(ring)+γ(CH)+ω (CH$_3$)	767.57	755.61
θ(ring)+ω $_{ring}$(CH)	702.5	704.33
ω $_{ring}$(CH)+ω $_{ring}$(NH)+δ(CH)	621.27	628.32
ω $_{ring}$(CH)+ω(NH)+θ(ring)	606.65	600.64
ω(NH)+θ(ring)	572.53	567.28

[a] ν, stretching; β, bending; α, scissoring; γ , rocking; ω, wagging; δ, twisting; θ, ring breathing; s, symmetric; as, asymmetric

^{13}C -NMR spectra of the title compound show the signals at 148.49 and 154.88 ppm due to C8 and C9 atoms of the triazole ring, respectively. These signals have been calculated as 140.34 and 145.07 ppm, respectively. The chemical shift values of C15 and C16 atoms bounded OCH3 group are observed as 146.19 and 147.36 ppm, whereas the corresponding values are 142.89 and 143.74 ppm for B3LYP level, respectively. While the C atoms of methoxy group belonging to the phenyl ring are observed at 55.32 ppm, the aliphatic CH2 (C7, C10, and C11) carbons are observed at 42.01, 33.42, and 31.16 ppm, respectively. The other calculated chemical shift values can be seen in Table 4. As can be seen from Table 4, theoretical ^{1}H and ^{13}C chemical shift results of the title compound are generally closer to the experimental ^{1}H and ^{13}C shift data.

**Frequencies
B3LYP/6-31G(d,p)
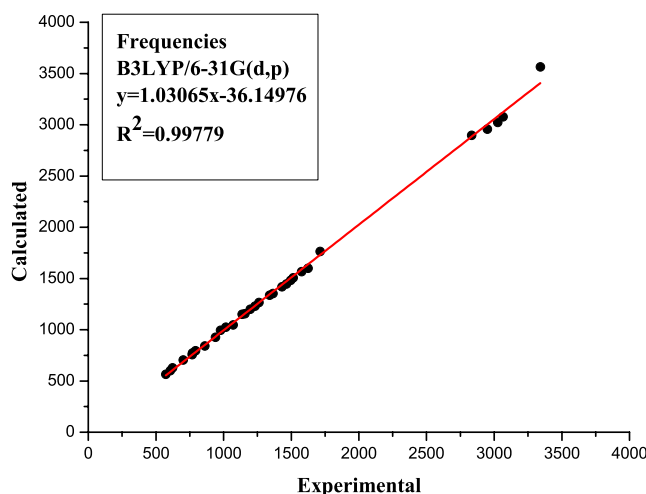y=1.03065x-36.14976
R^2=0.99779**

Fig. 4 Correlation graphics of calculated and experimental frequencies of the title compound

Table 4 Theoretical and experimental ^{1}H and ^{13}C isotropic chemical shifts (with respect to TMS, all values in ppm) for the title compound

Atom	Experimental (ppm) (DMSO-d$_6$)	Calculated (ppm) 6-31G(d,p) B3LYP
C1	-	123.52
C2	128.55	124.11
C3	126.83	121.73
C4	128.51	122.67
C5	-	123.82
C6	137.27	133.04
C7	42.01	35.67
C8	148.49	140.34
C9	154.88	145.07
C10	33.42	47.42
C11	31.16	35.67
C12	130.05	125.08
C13	120.50	116.12
C14	112.18	105.56
C15	146.19	142.89
C16	147.36	143.74
C17	111.67	106.83
C18	55.32	52.47
C19	55.32	52.83
H1	7.15–7.35	7.58
H2	7.15–7.35	7.52
H3	7.15–7.35	7.42
H4	7.15–7.35	7.42
H5	7.15–7.35	7.42
H6	3.56	3.36
H7	3.56	3.95
H8	-	7.38
H9	3.56	3.95
H10	3.56	3.06
H11	2.5	1.30
H12	2.5	3.06
H13	6.57–6.59	6.83
H14	6.85	6.45
H17	6.57–6.59	5.64
H18	3.71	3.48
H19	3.71	3.95
H20	3.71	3.48
H21	3.71	3.48
H22	3.71	3.95
H23	3.71	3.36

Molecular electrostatic potential

Molecular electrostatic potential (MEP) is related to the electronic density and is a very useful descriptor in understanding sites for electrophilic and nucleophilic

reactions as well as hydrogen bonding interactions [61–63]. The electrostatic potential $V(r)$ are also well suited for analyzing processes based on the "recognition" of one molecule by another, as in drug-receptor, and enzyme-substrate interactions, because it is through their potentials that the two species first "see" each other [64, 65]. Being a real physical property $V(r)s$ can be determined experimentally by diffraction or by computational methods [66].

To predict reactive sites for electrophilic and nucleophilic attack for the title molecule, MEP was calculated at the B3LYP/6-31G(d,p) optimized geometry. The negative (red color) regions of MEP were related to electrophilic reactivity and the positive (blue color) ones to nucleophilic reactivity shown in Fig. 5. As easily can be seen in Fig. 5, this molecule has several possible sites for electrophilic attack. The negative regions are mainly over the O1 atom and the region between O2 and O3 atoms. Also, a negative electrostatic potential region is observed around the N3 atom. The most negative $V(r)$ value is associated with O1 atom with a value −0.059 a.u. while the region between O2 and O3 atoms the value is about −0.050 a.u. However, a maximum positive region is localized on the N-H bond with a value of +0.044 a.u. indicating a possible site for nucleophilic attack. According to these calculated results, the MEP map shows that the negative potential sites are on electronegative atoms as well as the positive potential sites are around the hydrogen atoms. These sites give information about the region from where the compound can have intermolecular interaction and metallic bonding.
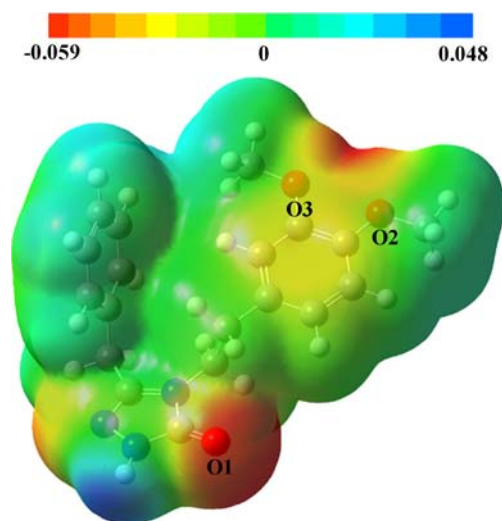

Fig. 5 Molecular electrostatic potential map calculated at B3LYP/6-31G(d,p) level

Table 5 Selected natural bond orbital occupancies of the title compound

NBO	Occupancies (a.u.)	NBO	Occupancies (a.u.)
BD (1) C5 - C4	1.97924	BD* (1) C5 - C4	0.01490
BD (1) C5 - C6	1.97587	BD* (1) C5 - C6	0.02162
BD (2) C5 - C6	1.66407	BD* (2) C5 - C6	0.34788
BD (1) C4 - C3	1.98078	BD* (1) C4 - C3	0.01572
BD (2) C4 - C3	1.66804	BD* (2) C4 - C3	0.33117
BD (1) C3 - C2	1.98096	BD* (1) C3 - C2	0.01574
BD (1) C2 - C1	1.97948	BD* (1) C2 - C1	0.01464
BD (2) C2 - C1	1.66558	BD* (2) C2 - C1	0.31856
BD (1) C1 - C6	1.97492	BD* (1) C1 - C6	0.02316
BD (1) C6 - C7	1.97109	BD* (1) C6 - C7	0.02688
BD (1) C7 - C8	1.97513	BD* (1) C7 - C8	0.02641
BD (1) C8 - N1	1.98401	BD* (1) C8 - N1	0.04604
BD (1) C8 - N3	1.98360	BD* (1) C8 - N3	0.01569
BD (2) C8 - N3	1.94282	BD* (2) C8 - N3	0.31130
BD (1) C9 - N1	1.97877	BD* (1) C9 - N1	0.10191
BD (1) C9 - N2	1.99062	BD* (1) C9 - N2	0.09386
BD (1) C9 - O1	1.99629	BD* (1) C9 - O1	0.44063
BD (2) C9 - O1	1.99437	BD* (2) C9 - O1	0.01525
BD (1) C10 - C11	1.97355	BD* (1) C10 - C11	0.02532
BD (1) C10 - N1	1.98535	BD* (1) C10 - N1	0.02644
BD (1) C11 - C12	1.97409	BD* (1) C11 - C12	0.01963
BD (1) C12 - C13	1.97532	BD* (1) C12 - C13	0.02212
BD (2) C12 - C13	1.70436	BD* (2) C12 - C13	0.35032
BD (1) C12 - C17	1.97067	BD* (1) C12 - C17	0.02206
BD (1) C13 - C14	1.97428	BD* (1) C13 - C14	0.01367
BD (1) C14 - C15	1.97926	BD* (1) C14 - C15	0.02491
BD (2) C14 - C15	1.70554	BD* (2) C14 - C15	0.38359
BD (1) C15 - C16	1.96910	BD* (1) C15 - C16	0.03242
BD (1) C15 - O2	1.99084	BD* (1) C15 - O2	0.02582
BD (1) C16 - C17	1.97832	BD* (1) C16 - C17	0.02369
BD (2) C16 - C17	1.71077	BD* (2) C16 - C17	0.38132
BD (1) C16 - O3	1.99081	BD* (1) C16 - O3	0.02564
BD (1) C19 - O3	1.99253	BD* (1) C19 - O3	0.00796
BD (1) C18 - O2	1.99247	BD* (1) C18 - O2	0.00779
BD (1) N2 - N3	1.98077	BD* (1) N2 - N3	0.01511

Note. BD for 2-center bond and BD* for 2-center antibond, a serial number (1, 2, . . . if there is a single, double, . . . bond between the pair of atoms), and the atom(s) to which the NBO is affixed

Natural bond orbital analysis

Selected NBO occupancies at bond critical points for the title compound is listed in Table 5, which were calculated on the B3LYP/6-31G(d,p) optimized structure.

NBO analyses reveal that the O1=C9 bond and C8=N3 bond have the character of double bonds, which is evident by B3LYP method. In benzyl and dimethoxyphenyl rings, the C-C bonds are typical single-double arrangement, which form the conjugate structure. The NBO occupancies of N1-C10 bond are larger than those of C7-C8 bond, indicating that the strength of bond N1-C10 is stronger than that of C7-C8 bond. All the results predicted here are consistent with the information obtained from the bond distances of the crystal structure. As the results coincide more with X-ray structure, NBO analysis can be a very useful method for molecular modeling.

Frontier molecular orbitals

The frontier molecular orbitals play an important role in the electric and optical properties, as well as in UV-Vis spectra and chemical reactions [67]. Figure 6 shows the distributions and energy levels of the HOMO-1, HOMO, LUMO, and LUMO+1 orbitals computed at the B3LYP/6-31G(d,p) level for the title compound. As seen from Fig. 6, in the
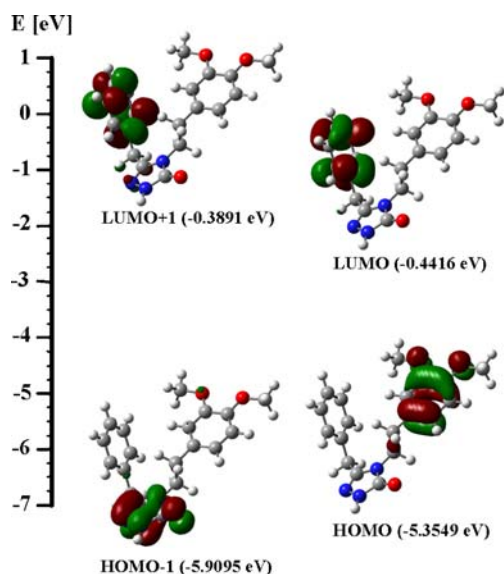
Fig. 6 HOMO and LUMO of the title compound

LUMO+1 and LUMO, electrons are mainly delocalized on the phenyl ring; in the HOMO-1, electrons are delocalized on O1 atom and triazole ring and in the HOMO, apart from the dimethoxyphenyl ring, electrons are also delocalized on O2 and O3 atoms. Both the highest occupied molecular orbitals (HOMOs) and the lowest-lying unoccupied molecular orbitals (LUMOs) are mainly localized on the rings indicating that the HOMO-LUMO are mostly the π-antibonding type orbitals. The value of the energy separation between the HOMO and LUMO is 4.9133 eV. This large HOMO-LUMO gap automatically means high excitation energies for many of excited states, a good stability and a high chemical hardness for the title compound.

Thermodynamic properties

On the basis of vibrational analysis and statistical thermodynamics, the standard thermodynamic functions: heat capacity ($C_{p,m}^0$), entropy (S_m^0), and enthalpy (H_m^0) were obtained at B3LYP/6-31G(d,p) level and listed in Table 6.

Table 6 shows that the standard heat capacities, entropies, and enthalpies increase at any temperature from

200.00 to 500.00 K, because the intensities of molecular vibration increase with the increasing temperature.

The correlation equations between these thermodynamic properties and temperature T are as follows:

$$C_{p,m}^0 = -0.20836 + 0.33801\,T - 1.13345 \times 10^{-4}\,T^2,$$
$$(R^2 = 0.99974)$$

(2)

$$S_m^0 = 73.32142 + 0.34648\,T - 6.10688 \times 10^{-5}\,T^2,$$
$$(R^2 = 1)$$

(3)

$$H_m^0 = -0.29493 + 0.01397\,T + 1.30913 \times 10^{-4}\,T^2,$$
$$(R^2 = 0.99999).$$

(4)

These equations will be helpful for further studies of the title compound.

Conclusions

5-benzyl-4-(3,4-dimethoxyphenethyl)-2H-1,2,4-triazol-3 (4H)-one has been synthesized and characterized by IR, NMR, and X-ray single-crystal diffraction. The calculated results show that the optimized geometries can well reproduce the crystal structure and the theoretical vibrational frequencies, and chemical shift values show good agreement with experimental results. Molecular electrostatic potential map shows several possible sites for electrophilic attack. Namely, the title compound can act as multidentate ligand to bind one or two metal centers, so resulting in interesting metal complexes with different coordination geometries. The value of the energy separation between the HOMO and LUMO is very large and this energy gap gives significant informations about the title compound. The NBO analysis are more compatible with the crystal structure of the title compound and it is a very useful method for molecular modeling. The correlations between the thermodynamic properties $C_{p,m}^o$, S_m^o, H_m^o, and temperatures T are also obtained.

Table 6 Thermodynamic properties at different temperatures at B3LYP/6-31G(d,p) level	T (K)	$H_m^0\ (kcal.mol^{-1})$	$C_{p,m}^0\ (cal.mol^{-1}.K^{-1})$	$S_m^0\ (cal.mol^{-1}.K^{-1})$
	200	7.765	63.277	140.157
	250	11.365	76.838	156.167
	298.15	15.482	90.205	171.193
	300	15.653	90.718	171.765
	350	20.632	104.365	187.087
	400	26.276	117.298	202.143
	450	32.544	129.240	216.892
	500	39.381	140.095	231.290

References

1. Zhang Y, Guo ZJ, You XZ (2001) J Am Chem Soc 123:9378–9387
2. Proft FD, Geerlings P (2001) Chem Rev 101:1451–1464
3. Fitzgerald G, Andzelm J (1991) J Phys Chem 95:10531–0534
4. Ziegler T (1991) Pure Appl Chem 63:873–878
5. Andzelm J, Wimmer E (1992) J Chem Phys 96:1280–1303
6. Scuseria GE (1992) J Chem Phys 97:7528–7530
7. Dickson RM, Becke AD (1993) J Chem Phys 99:3898–3905
8. Johnson BG, Gill PMW, Pople JA (1993) J Chem Phys 98:5612–5626
9. Oliphant N, Bartlett RJ (1994) J Chem Phys 100:6550–6561
10. Bhat AR, Bhat GV, Shenoy GG (2001) J Pharm Pharmacol 53:267–272
11. Al-Soud Yassen A, Al-Dweri Mohammad N, Al-Masoudi Najim A (2004) Il Farmaco 59:775–783
12. Demirbas N, Ugurluoglu R, Demirbas A (2002) Bioorg Med Chem 10:3717–3723
13. Emilsson H, Salender H, Gaarder J (1985) Eur J Med Chim Ther 21:333–338
14. Tozkoparan B, Gökhan N, Aktay G, Yesilada E, Ertan M (2000) Eur J Med Chem 35:743–750
15. Turan-Zitoui G, Kaplancikli ZA, Erol K, Kilic FS (1999) Il Farmaco 54:218–223
16. Katica CR, Vesna D, Vlado K, Dora GM, Aleksandra B (2001) Molecules 6:815–824
17. Kaszuwara W, Leonowicz M, Ukasiewicz A (1992) Mater Lett 12:429–433
18. Prins R, Biagini-Cingi M, de Graaff RAG, Haasnoot J, Manotti-Lanfredi AM, Rabu P, Reedijk J, Ugozzoli F (1996) Inorg Chim Acta 248:35–44
19. Drabent K, Biaoska A, Ciunik Z (2004) Inorg Chem Commun 7:224–227
20. Lyakhov AS, Vorobiov AN, Gaponik PN, Ivashkevich LS, Matulis VE, Ivashkevich OA (2003) Acta Cryst C 59:o690–693
21. Jia LH, Liu ZL, Liu W (2007) Acta Cryst E 63:o2766
22. Sorescu DC, Bennett CM, Thompson DL (1998) J Phys A 102:10348–10357
23. Palmer MH, Christem D (2004) J Mol Struct 705:177–187
24. Jimenez V, Alderete JB (2006) J Mol Struct (Theochem) 775:1–7
25. El-Azhary AA, Suter HU, Kubelka J (1998) J Phys Chem A 102:620–629
26. Da Silva G, Moore EE, Bozzelli JW (2006) J Phys Chem A 110:13979–13988
27. Matulis VE, Ivashkevich OA, Gaponik PN, Elkind PD, Sukhanov GT, Bazyleva AB, Zaitsau DH (2008) J Mol Struct (Theochem) 854:18–25
28. Billes F, Endredi H, Keresztury G (2000) J Mol Struct (Theochem) 530:183–200
29. Krishnakumar V, Xavier RJ (2004) Spectrochim Acta A 60:709–714
30. Zaza S, Guedira F, Zaydoun S, Saidi Idrissi M, Lautie A, Romain F (2004) Can J Anal Sci Spectrosc 49:15–23
31. Krishnakumar V, Keresztury G, Sundius T, Xavier RJ (2005) Spectrochim Acta A 61:261–267
32. Pagacz-Kostrzewa M, Bronisz R, Wierzejewska M (2009) Chem Phys Lett 473:238–246
33. Pitucha M, Borowski P, Karczmarzyk Z, Fruzinski A (2009) J Mol Struct 919:170–177
34. Sanchez-Soto PJ, Morillo E, Perez-Rodriguez JL, Real C (1995) J Therm Anal 45:1189–1197
35. Li J, Litzinger TA (2007) Thermochim Acta 454:116–127
36. Badea M, Olar R, Marinescu D, Vasile G (2008) J Therm Anal Calorim 92:209–214
37. Kumar NV, Mashelkar UC (2007) Heterocycl Commun 13:211
38. Perez-Castro I, Caamano O, Fernandez F, Garcia MD, Lopez C, De Clercq E (2007) Org Biomol Chem 5:3805–3813
39. Bekirarcan O, Bektas H (2006) Molecules 11:469–477
40. Haasnoot JG (2000) Coord Chem Rev 131:200–202
41. Li W, Jia HP, Ju ZF, Zhang J (2006) Cryst Growth Des 6:2136–2140
42. Chen Z, Li X, Liang F (2008) J Solid State Chem 181:2078–2086
43. Lin YY, Zhang YB, Zhang JP, Chen XM (2008) Cryst Growth Des 8:3673–3679
44. Van Koningsbruggen PJ (2004) Top Curr Chem 233:123–149
45. Bronisz R (2005) Inorg Chem 44:4463–4465
46. Frisch MJ, Trucks GW, Schlegel HB, Scuseria GE, Robb MA, Cheeseman JR, Montgomery JA Jr, Vreven T, Kudin KN, Burant JC, Millam JM, Iyengar SS, Tomasi J, Barone V, Mennucci B, Cossi M, Scalmani G, Rega N, Petersson GA, Nakatsuji H, Hada M, Ehara M, Toyota K, Fukuda R, Hasegawa J, Ishida M, Nakajima T, Honda Y, Kitao O, Nakai H, Klene M, Li X, Knox JE, Hratchian HP, Cross JB, Bakken V, Adamo C, Jaramillo J, Gomperts R, Stratmann RE, Yazyev O, Austin AJ, Cammi R, Pomelli C, Ochterski JW, Ayala PY, Morokuma K, Voth GA, Salvador P, Dannenberg JJ, Zakrzewski VG, Dapprich S, Daniels AD, Strain MC, Farkas O, Malick DK, Rabuck AD, Raghavachari K, Foresman JB, Ortiz JV, Cui Q, Baboul AG, Clifford S, Cioslowski J, Stefanov BB, Liu G, Liashenko A, Piskorz P, Komaromi I, Martin RL, Fox DJ, Keith T, Al-Laham MA, Peng CY, Nanayakkara A, Challacombe M, Gill PMW, Johnson B, Chen W, Wong MW, Gonzalez C, Pople JA (2004) Gaussian 03 Revision E01. Gaussian Inc, Wallingford, CT
47. Merrick JP, Moran D, Radom L (2007) J Phys Chem A 111:11683–11700
48. Frisch A, Dennington R II, Keith T, Millam J, Nielsen AB, Holder AJ, Hiscocks J (2007) GaussView Reference Version 40. Gaussian Inc, Pittsburgh
49. Ditchfield R (1972) J Chem Phys 56(11):5688–5691
50. Wolinski K, Hinton JF, Pulay P (1990) J Am Chem Soc 112 (23):8251–8260
51. Politzer P, Murray J (2002) Theor Chem Acc 108:134–142
52. Farrugia LJ (1997) J Appl Crystallogr 30:565
53. Hanif M, Qadeer G, Rama NH, Akhtar J, Helliwell M (2009) Acta Cryst E65:o387
54. Köysal Y, Işık Ş, Doğdaş E, Tozkoparan B, Ertan M (2004) Acta Cryst C60:o356–357
55. Sancak K, Ustabaş R, Çoruh U, Er M, Ünver Y, Yavuz M (2005) Acta Cryst E61:o1764–1766
56. Ünver Y, Ustabaş R, Çoruh U, Sancak K, Vazquez-Lopez EM (2006) Acta Cryst E62:o3938–3939
57. Zhao PS, Xu JM, Zhang WG, Jian FF, Zhang L (2007) Struct Chem 18:993–1000
58. Genç S, Dege N, Çetin A, Cansız A, Şekerci M, Dinçer M (2004) Acta Cryst E60:o1339–1341
59. Dinçer M, Avcı D, Şekerci M, Atalay Y (2008) J Mol Model 14:823–832
60. Vainilavicius P, Smicius R, Jakubkiene V, Tumkevicius S (2001) Manatshefte für Chemie 132:825–831
61. Scrocco E, Tomasi J (1978) Adv Quantum Chem 11:115–121
62. Luque FJ, Lopez JM, Orozco M (2000) Theor Chem Acc 103:343–345
63. Okulik N, Jubert AH (2005) Internet Electron J Mol Des 4:17–30
64. Politzer P, Laurence PR, Jayasuriya K, McKinney J (1985) Special issue of Environ Health Perspect 61:191–202
65. Scrocco E, Tomasi J (1973) Topics in current chemistry, vol 7. Springer, Berlin, p 95
66. Politzer P, Truhlar DG (1981) Chemical applications of atomic and molecular electrostatic potentials. Plenum, New York
67. Fleming I (1976) Frontier orbitals and organic chemical reactions. Wiley, London